Cell Proliferation
Cell Prolif. 2008, **41**, 607–624 doi: 10.1111/j.1365-2184.2008.00541.x

An efficient experimental strategy for mouse embryonic stem cell differentiation and separation of a cytokeratin-19-positive population of insulin-producing cells

O. Naujok*, F. Francini*, A. Jörns*† and S. Lenzen*

*Institute of Clinical Biochemistry and †Center of Anatomy, Hannover Medical School, Hannover, Germany

Received 30 *August* 2007; *accepted* 21 *November* 2007

Abstract. *Objectives*: Embryonic stem cells are a potential source for insulin-producing cells, but existing differentiation protocols are of limited efficiency. Here, the aim has been to develop a new one, which drives development of embryonic stem cells towards insulin-producing cells rather than to neuronal cell types, and to combine this with a strategy for their separation from insulin-negative cells. *Materials and methods*: The cytokeratin-19 (CK19) promoter was used to control the expression of enhanced yellow fluorescence protein in mouse embryonic stem cells during their differentiation towards insulin-producing cells, using a new optimized four-stage protocol. Two cell populations, $CK19^+$ and $CK19^-$ cells, were successfully fluorescence sorted and analysed. *Results*: The new method reduced neuronal progeny and suppressed differentiation into glucagon- and somatostatin-producing cells. Concomitantly, β-cell like characteristics of insulin-producing cells were strengthened, as documented by high gene expression of the Glut2 glucose transporter and the transcription factor Pdx1. This novel protocol was combined with a cell-sorting technique. Through the combined procedure, a fraction of glucose-responsive insulin-secreting $CK19^+$ cells was obtained with 40-fold higher insulin gene expression and 50-fold higher insulin content than $CK19^-$ cells. $CK19^+$ cells were immunoreactive for C-peptide and had ultrastructural characteristics of an insulin-secretory cell. *Conclusion*: Differentiated $CK19^+$ cells reflect an endocrine precursor cell type of ductal origin, potentially suitable for insulin replacement therapy in diabetes.

INTRODUCTION

The differentiation protocol by Lumelsky *et al*. (2001), originally established to differentiate mouse embryonic stem cells (ESCs) into neuronal cells (Lee *et al*. 2000), has also been a reference tool for differentiation of mouse ESCs towards insulin-producing cells; however, its efficiency is low (Paek *et al*. 2005). Various other alternative mouse ESC differentiation methods have been developed, but the results of these activities have also been disappointing, due to limited efficiency and reproducibility (Soria *et al*. 2000; Hori *et al*. 2002). The yield of insulin-

Correspondence: Sigurd Lenzen, Institute of Clinical Biochemistry, Hannover Medical School, D-30623 Hannover, Germany. E-mail: clinbiochemistry@mh-hannover.de

producing cells is usually so low that the amount of insulin they produce cannot be reliably quantified, in particular when tissue culture media contain insulin (Rajagopal *et al*. 2003; Hansson *et al*. 2004). Thus, it has been doubted whether cells obtained during the course of such experiments may be suited for reproducible generation of insulin-producing cells (Sipione *et al*. 2004). With a few exceptions (Soria *et al*. 2000; Leon-Quinto *et al*. 2004; Roche *et al*. 2005; Vaca *et al*. 2006), work on ESC differentiation towards insulin-producing cells has been focused on variation of cell culture conditions (Lumelsky *et al*. 2001; Hori *et al*. 2002; Moritoh *et al*. 2003; Bai *et al*. 2005; Shi *et al*. 2005) or overexpression of transcription factors that are known to be important for pancreatic organogenesis (Blyszczuk *et al*. 2003; Miyazaki *et al*. 2004; Shiroi *et al*. 2005). However, none of these have been suited to separate insulin-producing cells from other cell types, which also develop during differentiation.

In Lumelsky *et al*.'s original method, the idea was put forward that ESCs may differentiate *in vitro* into nestin-positive endocrine precursor cells that would differentiate further towards insulin-producing cells. This approach was based on the assumption that β-cell neogenesis in the pancreas results from differentiation of nestin-positive cells, as such a population is resident in adult pancreas (Hunziker & Stein 2000; Zulewski *et al*. 2001). However, participation of nestin-positive cells in β-cell regeneration is doubtful (Selander & Edlund 2002; Treutelaar *et al*. 2003). In addition to nestin-positive cells, another cell population, namely cytokeratin-19-positive ($CK19^+$) ductal cells, have been considered to be a pool for newly derived β-cells during pancreatic organogenesis (Rutter 1980; Slack 1995; Bouwens *et al*. 1997; Bonner-Weir *et al*. 2000; Bouwens & Rooman 2005). In the mouse, pancreatic primordia develop from the primitive gut tube stage after gastrulation, from a Pdx1-expressing cell population (Edlund 2002). The pancreas at this stage exists as separate dorsal and ventral buds, which grow in size and later fuse to form the definitive pancreatic tissue. In contrast, several studies have doubted the hypothesis of neuroectodermal origin of the β-cells, and that pancreatic endocrine cells may develop from duct-like cells that migrate into the surrounding mesenchyme and differentiate into the four major hormone-expressing cell types (Rutter 1980). Most importantly, these transitional cells would express CK19 and co-express insulin (Bouwens & De Blay 1996; Bouwens *et al*. 1997; Bouwens & Pipeleers 1998). Such ductal cells have shown capacity to proliferate and differentiate *in vitro* into islet cells (Bonner-Weir *et al*. 2000; Gao *et al*. 2003, 2005). Moreover, re-expression of β-cell specific transcription factor Pdx1 has been observed in ductal cells when placed in cell culture, indicating an early endocrine precursor cell type (Gmyr *et al*. 2000). In addition to these findings, participation of CK19 during differentiation towards insulin-producing cells has been observed in mouse (Blyszczuk *et al*. 2004) and recently in human (Jiang *et al*. 2007) embryonic stem cell lines. Not surprisingly, appearance of $CK19^+$ cells in ESCs undergoing *in vitro* differentiation towards insulin-producing cells reflects a mechanism analogous to that described for differentiation of ductal tissue into insulin-producing cells during foetal development of the pancreas (Gao *et al*. 2003; Noguchi *et al*. 2003; Bonner-Weir *et al*. 2004). However, efficient generation of insulin-producing cells from ESCs requires not only a reliable differentiation method, but in addition a sensitive cell separation strategy. To overcome the drawbacks of the reference protocol, we have established a new straightforward and optimized four-stage strategy that minimizes neuronal differentiation potential and suppresses differentiation into glucagon- and somatostatin-producing cells. We have combined this with a cell-sorting technique based on fluorescence-activated cell sorter (FACS) analysis. Specifically, the CK19 promoter was used to control expression of enhanced yellow fluorescence protein (eYFP) in mouse ESCs during their differentiation towards insulin-producing cells. Two distinct cell populations, $CK19^+$ and $CK19^-$ cells, were successfully separated and analysed. This approach yielded an insulin-producing cell type from $CK19^+$ endocrine precursors.

MATERIALS AND METHODS

Materials

Dulbecco's modified Eagle's medium (DMEM) and DMEM/F-12 tissue culture media, glutamine, non-essential amino acids and basic fibroblast growth factor (bFGF) were obtained from Invitrogen (Karlsruhe, Germany). Foetal calf serum (FCS) embryonic stem cell grade and gentamicin were purchased from PAA (Vienna, Austria) and leukaemia inhibitory factor (LIF) from Chemicon (Temecula, CA, USA). Insulin, transferrin, sodium selenite, putrescine and progesterone were from Sigma (St. Louis, MO, USA). All primer pairs, including random hexamer primers, were synthesized by MWG (Munich, Germany). The RevertAid™ H Minus M-MuLV Reverse Transcriptase was from Fermentas (St. Leon-Rot, Germany). Biotherm™ Taq polymerase as well as the deoxynucleoside triphosphates were from Genecraft (Münster, Germany). SYBR Green I was from Biozym (Hess. Oldendorf, Germany) and plastic ware for real-time polymerase chain reaction (PCR) reactions were from Abgene (Hamburg, Germany). C-peptide antibody was from Linco Research (St. Charles, MS, USA) and insulin antibody from Abcam (Cambridge, UK). Secondary antibodies were provided by Dianova (Hamburg, Germany). Unless otherwise mentioned, chemicals of analytical grade were obtained from Sigma or Merck (Darmstadt, Germany).

Plasmid construction and transfection

The pGL3-CK19 backbone vector was kindly provided by Dr. Shuichi Kaneko (Kanazawa University, Kanazawa, Japan). The luciferase sequence downstream of the 2.9 kb CK19 promoter fragment was removed by DNA digestion with *Hin*dIII and *Xba*I. Subsequently, cDNA of eYFP was purified by DNA digestion from the pEYFP-N1 vector (Clontech, Mountain View, CA, USA) as described above and was subcloned into the linearized pGL3-CK19 vector. In the obtained gene cassette, the human CK19 promoter drives the expression of eYFP followed by a poly(A) signal. ES-D3 cells were co-transfected with pCK19-eYFP and pCDNA3 plasmid featuring a neomycin gene for cell selection. Cell transfections were performed with Effectene (Qiagen, Hilden, Germany) according to the manufacturer's instructions. Resistant clones were selected, using 300 μg/mL G418, and successful integration of the construct was verified by RT-PCR from genomic DNA. Five different YFP clones were generated and on the basis of analysis of fluorescence intensity, the best clone was selected for detailed analyses in the present study. Resulting transgenic embryonic stem cells were designated ES-D3 CK19-eYFP.

Cell lines and culture conditions

The mouse embryonic stem cell line ES-D3 (Doetschman *et al*. 1985) was purchased from the American Tissue Culture Collection (Manassas, VA, USA). These cells were differentiated towards insulin production using a new four-stage differentiation protocol and results were compared to those of a previously published method (Lumelsky *et al*. 2001). In order to maintain the cells in an embryonic state, they were cultured on a feeder layer of mouse embryonic fibroblasts in DMEM containing 25 mM glucose and supplemented with 15% (v/v) FCS, 2 mM L-glutamine, 100 μM non-essential amino acids, 0.1 mM β-mercaptoethanol, 50 μg/mL gentamicin and 1000 U/mL LIF in a humidified atmosphere at 37 °C and 5% CO_2. Medium was changed every day. Subsequently, the cells were transferred for two passages on to gelatin-coated tissue culture dishes to remove them from the feeder layer.

For differentiation with the new protocol, the cells were trypsinized and counted using a haemocytometer. One million cells were transferred to a bacterial culture dish in medium, as

described above, but devoid of LIF. Cells were then grown for up to 5 days in suspension. During this time, embryoid bodies formed that were allowed to settle on to gelatin-coated dishes in serum-free DMEM/F-12 medium supplemented with 25 μg/mL insulin, 50 μg/mL transferrin, 30 nM sodium selenite, 20 nM progesterone, 100 μM putrescine, 2 mM L-glutamine, 100 μM non-essential amino acids and 10 ng/mL bFGF, for 14 days. Thereafter, the cells were cultured for 7 days in DMEM/F-12 medium supplemented with 25 μg/mL insulin, 50 μg/mL transferrin, 30 nM sodium selenite, 20 nM progesterone, 100 μM putrescine, 5% FCS, 2 mM L-glutamine, 1× non-essential amino acids and 10 mM nicotinamide.

FACS analysis and cell sorting

ES-D3 CK19-eYFP cells at different time points along the new differentiation protocol were trypsinized, centrifuged and re-suspended in Krebs–Ringer buffer supplemented with 1 mM EDTA and 20% FCS. They were then filtered through a 40-μM gauze and sorted on a MoFlo cell sorter into $CK19^+$ and $CK19^-$ cell populations (DakoCytomation, Fort Collins, CO, USA).

Molecular biology

Total RNA was isolated from ESCs using the Chomczynski system (Chomczynski & Sacchi 1987). RNA was quantified photometrically and analysed on a denaturing agarose gel. For cDNA synthesis, random hexamers were used to prime the reaction of RevertAid™ H Minus M-MuLV reverse transcriptase. QuantiTect SYBR Green™ technology (Qiagen, Hilden, Germany), which uses a fluorescent dye that binds only double-stranded DNA, was employed. Reactions were performed using DNA Engine Opticon™ Sequence Detection System (Biozym Diagnostik, Hess. Oldendorf, Germany). Samples were first denatured at 94 °C for 3 min followed by 40 PCR cycles. Each cycle comprised a melting step at 94 °C for 30 s, an annealing step at 62 °C for 30 s, and an extension step at 72 °C for 30 s. Each PCR amplification was performed in triplicate using primers for insulin (detecting both Ins1 and Ins2), glucagon, somatostatin, nestin, Glut2, Pdx1, Nkx6.1, Kir6.2, Sur1, glucokinase, Oct4, neural cell adhesion molecule (NCAM), β-actin, CK19, carbonic anhydrase 2, amylase 2 and albumin (Table 1). Optimal parameters for PCRs were empirically defined. Purity of amplified PCR products was verified by melting curves. Data are expressed as relative gene expressions after normalization to the β-actin housekeeping gene using *Qgene96* and *LineRegPCR* software (Muller *et al*. 2002; Ramakers *et al*. 2003).

Ultrastructural characterization

For electron microscopy, cell pellets of ESCs and MIN6 cells (Miyazaki *et al*. 1990) were fixed in 2% paraformaldehyde plus 2% glutaraldehyde in 0.1 M cacodylate buffer, pH 7.3 and were post-fixed in 1% OsO_4 then finally embedded in Epon resin. Ultrathin sections were contrast-stained with saturated solutions of lead citrate and uranyl acetate and were viewed by electron microscopy (Gurgul *et al*. 2004).

Immunostaining and microscopy

Immunocytochemical co-staining for C-peptide and insulin was performed according to standard procedures. $0.5–1 \times 10^4$ FACS-sorted ESCs and MIN6 cells as positive controls were seeded overnight on glass slides and then fixed in 4% paraformaldehyde for 30 min. Thereafter, cells were blocked for 20 min in phosphate-buffered saline (PBS) plus 0.2% Triton X-100, 1% bovine serum albumin (BSA) and 5% donkey serum. Incubation with anti-C-peptide antibody was performed at room temperature for 60 min, diluted 1 : 100 in PBS with 0.1% BSA followed by incubation with Cy5-conjugated secondary antibody diluted 1 : 500 in PBS + 0.1% BSA for 30 min. Incubation with anti-insulin antibody was also performed at room temperature for

Table 1. Primers used for qRT-PCR. All amplicons were designed exon-spanning and were in a size ranging from 100 to 300 bp

Gene		Primer sequence
Insulin	Fw	5′-CCCACCCAGGCTTTTGTCAAACAGC-3′
	Rv	5′-TCCAGCTGGTAGAGGGAGCAGATG-3′
Glucagon	Fw	5′-CAGGGCACATTCACCAGCGACTAC-3′
	Rv	5′-TCAGAGAAGGAGCCATCAGCGTG-3′
Somatostatin	Fw	5′-ATGCTGTCCTGCCGTCTCCA-3′
	Rv	5′-TGCAGCTCCAGCCTCATCTCG –3′
Nestin	Fw	5′-GAGAGTCGCTTAGAGGTGCA-3′
	Rv	5′-CCACTTCCAGACTAAGGGAC-3′
Glut2	Fw	5′-GAAGACAAGATCACCGGAACCTTGG-3′
	Rv	5′-GGTCATCCAGTGGAACACCCAAAA-3′
Pdx1	Fw	5′-ACCGCGTCCAGCTCCCTTTC-3′
	Rv	5′-CAACATCACTGCCAGCTCCACC-3′
Nkx6.1	Fw	5′-AGAACCGCAGGACCAAGTGGAGAA-3′
	Rv	5′-TCGTCATCCTCCTCATTCTCCGAAG-3′
Kir6.2	Fw	5′-TGCTGTCCCGAAAGGGCATTATC-3′
	Rv	5′-TGCAGTTGCCTTTCTTGGACACG-3′
Sur1	Fw	5′-ACCAAGGTGTCCTCAACAACGGCT-3′
	Rv	5′-TGGAGCCAGGTGCTATGGTGAATG-3′
Glucokinase	Fw	5′-GAGGTCGGCATGATTGTGGGCA-3′
	Rv	5′-GCGCCCCACTCTGTGTTGACACAC-3′
Oct 4	Fw	5′-AGGCCCGGAAGAGAAAGCGAACTA-3′
	Rv	5′-TGGGGGCAGAGGAAAGGATACAGC-3′
NCAM	Fw	5′-CGACGAGGCCGAATACGTCTG-3′
	Rv	5′-GCTCCTCTAGTTCCATGGCCGTC-3′
β-Actin	Fw	5′-AGAGGGAAATCGTGCGTGAC-3′
	Rv	5′-CAATAGTGATGACCTGGCCGT-3′
Cytokeratin 19	Fw	5′-GGTGCCACCATTGACAACTC-3′
	Rv	5′-CTGCATCTCCAGGTCAGTCC-3′
Carbonic anhydrase 2	Fw	5′-CCACCACTGGGGATACAGCAAGC-3′
	Rv	5′-GTCCTCCTTTCAGCACTGCATTGTC-3′
Amylase 2	Fw	5′-CTGTGAACACAGATGGCGTCAAATC-3′
	Rv	5′-GCAGGAAGACCAGTCTGTAAAGTGGC-3′
Albumin	Fw	5′-CCTCCTCTTCGTCTCCGGCTCTG-3′
	Rv	5′-GGGATTTGTCACAGTTGGCGGC-3′

Fw, forward (sense) primer; Rv, reverse (antisense) primer; NCAM, neural cell adhesion molecule.

120 min diluted 1 : 100 in PBS with 0.1% BSA, followed by incubation with Texas Red or FITC-conjugated secondary antibody diluted 1 : 500 in PBS + 0.1% BSA for 30 min. Subsequently, the cells were washed and nuclei were counterstained with 300 nM 4′,6-diamidino-2-phenylindole (DAPI) for 5 min at room temperature. Finally, the cells were washed and mounted with Mowiol/DABCO antiphotobleaching mounting media. Stained cells were examined on an Olympus IX81 inverted microscope (Olympus, Hamburg, Germany) and microscopy images were post-processed with *AutoDeblur* and *AutoVisualize* (Autoquant Imaging, New York, USA).

Insulin secretion and insulin content

Cells were seeded at a density of 1×10^5/well in 48-well culture dishes and were grown for 24 h in DMEM/F-12 medium without insulin and supplemented with 5.5 mM glucose; they were then

washed with Krebs–Ringer buffer. Insulin secretion during a 120-min incubation period was measured in Krebs–Ringer buffer containing 0 mM and 30 mM glucose. After incubation, medium was removed and gently centrifuged to remove detached cells. Insulin was measured in the supernatant. For measurement of insulin content, cells were sonicated in Krebs–Ringer buffer. Insulin was determined by radioimmunoassay using rat insulin as standard.

Statistical analyses

Data are expressed as mean values ± SEM. Unless stated otherwise statistical analyses were performed using ANOVA followed by Bonferroni's test for multiple comparisons or *t*-test for paired correlations, using the Prism analysis program (GraphPad, San Diego, CA, USA).

RESULTS

Comparison of the gene expression profile after differentiation of ESCs according to the reference differentiation protocol or to the optimized four-stage differentiation protocol

Quantitative analysis of gene expression in mouse ESCs, which had been differentiated according to the reference protocol by Lumelsky *et al*. (2001), showed that all three major pancreatic endocrine hormones, insulin, glucagon and somatostatin were readily expressed. In contrast, ESCs differentiated according to the new optimized four-stage differentiation protocol expressed insulin almost exclusively, while glucagon expression was not detectable and somatostatin expression was low when compared to the reference protocol (Table 2, Fig. 1).

The structural marker genes *glucokinase*, *Kir6.2* and *Sur1*, which play a crucial role in β-cell stimulus-secretion coupling, were well expressed in cells from both protocols. In addition, expression of CK19 and carbonic anhydrase 2 (CA2), both markers for pancreatic duct cells, were increased significantly by 6-fold and 9-fold, respectively (Table 2). Interestingly, *Sur1*

Table 2. Comparison of the relative gene expression profile of unsorted mouse embryonic stem cells, comprising pancreatic hormones, transcription factors and structural markers, after differentiation into insulin-producing cells, according to the reference protocol by Lumelsky *et al*. (2001), or to the optimized four-stage differentiation protocol

	Reference protocol (%)	Optimized four-stage protocol (%)
Insulin	100 ± 24 (6)	136 ± 27 (13)
Glucagon	100 ± 32 (5)	n.d.
Somatostatin	100 ± 38 (5)	11 ± 4 (11)
Pdx1	100 ± 52 (4)	1184 ± 438 (13)
Glut2	100 ± 24 (4)	338 ± 98 (10)
Glucokinase	100 ± 24 (6)	122 ± 29 (10)
Kir6.2	100 ± 7 (4)	96 ± 24 (12)
Sur1	100 ± 23 (6)	182 ± 47 (10)
Nestin	100 ± 32 (4)	49 ± 12 (10)
NCAM	100 ± 20 (5)	16 ± 4 (6)
Carbonic anhydrase 2	100 ± 29 (4)	561 ± 103 (11)
Cytokeratin-19	100 ± 22 (5)	895 ± 81 (10)

Data shown are gene expression values determined by qPCR on day 26 of differentiation. Depicted are the changes in relative expression in percentage, normalized to the reference protocol by Lumelsky *et al*. (2001). Values shown are means ± SEM of the relative gene expression. n.d., not detectable; NCAM, neural cell adhesion molecule.

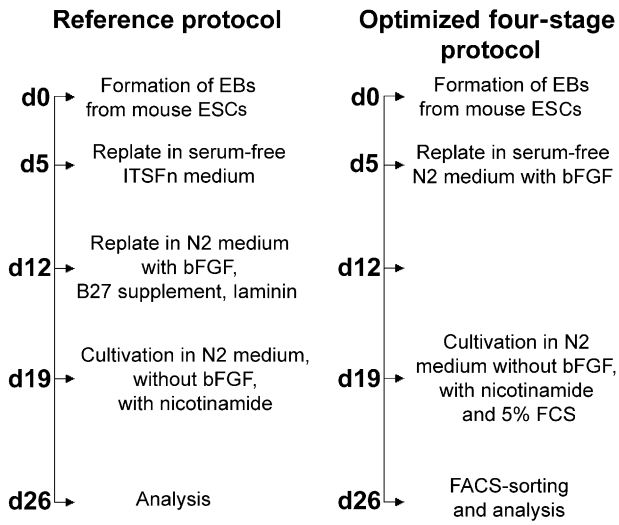

Figure 1. Comparative schematic presentation of the two different protocols used for differentiation of mouse embryonic stem cells (ESCs) into insulin-producing cells.

expression was nearly 2-fold higher in cells differentiated with the new four-stage protocol compared to the reference method (Table 2). The glucose transporter Glut2 and the transcription factor Pdx1 were both weakly expressed. Higher expression levels were observed for Glut2 glucose transporter and β-cell transcription factor Pdx1 after the new optimized four-stage protocol, with a 3-fold increase for Glut2 and 12-fold increase for Pdx1 (Table 2). Nestin and NCAM levels were measured to analyse differentiation towards neuronal progeny. They were both strongly expressed after the reference recipe, while cells from the new optimized four-stage differentiation protocol showed a 2-fold decrease in nestin and a 6-fold decrease in NCAM (Table 2). Gene expression analysis of amylase revealed only traces of mRNA expression in cells from the reference protocol, while in cells from the new optimized four-stage one amylase expression was undetectable (data not shown). Albumin expression, a marker for differentiation towards hepatic progeny, was negligible in both protocols with levels typically at or below the detection limit of real-time PCR (data not shown).

FACS sorting of CK19$^+$ and CK19$^-$ cells differentiated from mouse ESCs, according to the optimized four-stage differentiation protocol

The pCK19-eYFP construct was successfully integrated into ESCs. Cell clones could be selected and maintained in an undifferentiated state with identical morphology when compared to wild-type ESCs. Moreover, growth rate of transfected and non-transfected cells was comparable, indicating that their embryonic properties were not affected by transfection and subsequent selection process. Interestingly, undifferentiated clones displayed eYFP positivity (91.0 ± 0.6%, $n = 4$) that grossly decreased after formation of embryoid bodies to 13.4 ± 1.1% on day 5 ($n = 7$), 11.2 ± 1.2% on day 12 ($n = 10$), 6.8 ± 1.1% on day 19 ($n = 8$) and 1.6 ± 0.3% on day 26 ($n = 16$) of differentiation with the new optimized method (Fig. 2b). Analysis of gene expression of endogenous CK19 significantly revealed 4–7-fold higher CK19 expression in CK19$^+$ FACS-sorted cells when compared to CK19$^-$ cells (Fig. 2c). Carbonic anhydrase 2 was analysed as a

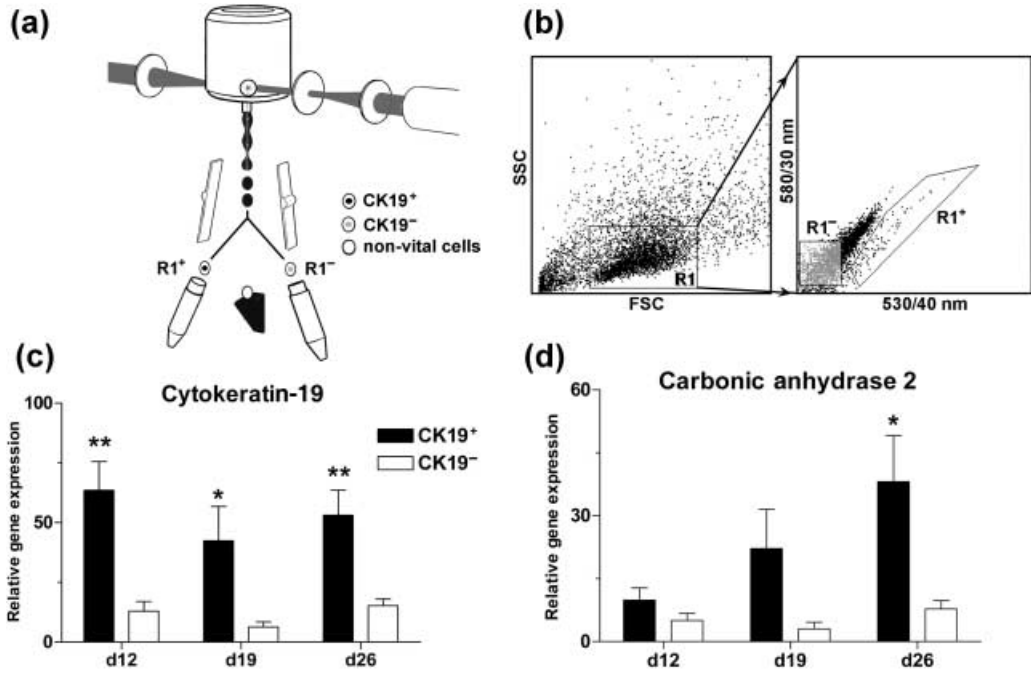

Figure 2. Selection of CK19$^+$ and CK19$^-$ cells through FACS sorting of insulin-producing cells differentiated from mouse embryonic stem cells (ESCs) according to the optimized four-stage differentiation protocol. (a) Schematic presentation of the method used for separation of vital CK19$^+$ and CK19$^-$ cells and non-vital cells by FACS sorting. (b) Clonal ESCs differentiated according to the optimized four-stage differentiation protocol were analysed with respect to size (FSC) and granularity (SSC) on day 26 of differentiation. Vital cells were gated (R1) and analysed for fluorescence intensity. CK19$^+$ (R1$^+$) and CK19$^-$ (R1$^-$) cells were separated. (c) Cytokeratin-19 gene expression in FACS-sorted CK19$^+$ and CK19$^-$ cells. Values shown are means ± SEM of the relative gene expression of 5–13 experiments; $*P < 0.05$, $**P < 0.01$. (d) Carbonic anhydrase 2 gene expression in FACS-sorted CK19$^+$ and CK19$^-$ cells. Values shown are means ± SEM of the relative gene expression of four to eight experiments; $*P < 0.05$. SSC, side scatter; FSC, forward scatter.

second marker for duct cell progeny. Analysis of gene expression showed a 2-fold increase in CK19$^+$ cells at day 12 and a significant 9-fold increase in expression in CK19$^+$ cells at day 26, when compared to CK19$^-$ cells (Fig. 2d).

Gene expression profiles of pancreatic hormones and transcription factors in CK19$^+$ and CK19$^-$ cells during differentiation from mouse ESCs

Quantitative analysis of gene expression revealed a low level of insulin in CK19$^+$ and CK19$^-$ cells up to day 19. A significant 80-fold increase in insulin gene expression was observed in CK19$^+$ cells on day 26 as compared to day 12 and day 19 (Fig. 3). Compared to CK19$^-$ cells, insulin gene expression on day 26 was higher by a factor of 38 (Fig. 3), whereas the level of insulin gene expression in CK19$^-$ cells did not change significantly. Glucagon gene expression was not detectable at day 12 and day 19 (Fig. 3), while glucagon gene expression remained barely detectable at day 26 in CK19$^+$ cells, it increased to appreciable levels in CK19$^-$ cells 12 times higher than in CK19$^+$ cells (Fig. 3). Somatostatin gene expression was marginal throughout the whole differentiation protocol at days 12, 19 and 26 in CK19$^+$ cells (Fig. 3). In CK19$^-$ cells, somatostatin gene expression was high at day 12 but had decreased by days 19 and 26 (Fig. 3). Nevertheless, the expression level was seven times higher than in CK19$^+$ cells (Fig. 3). Thus, CK19$^+$

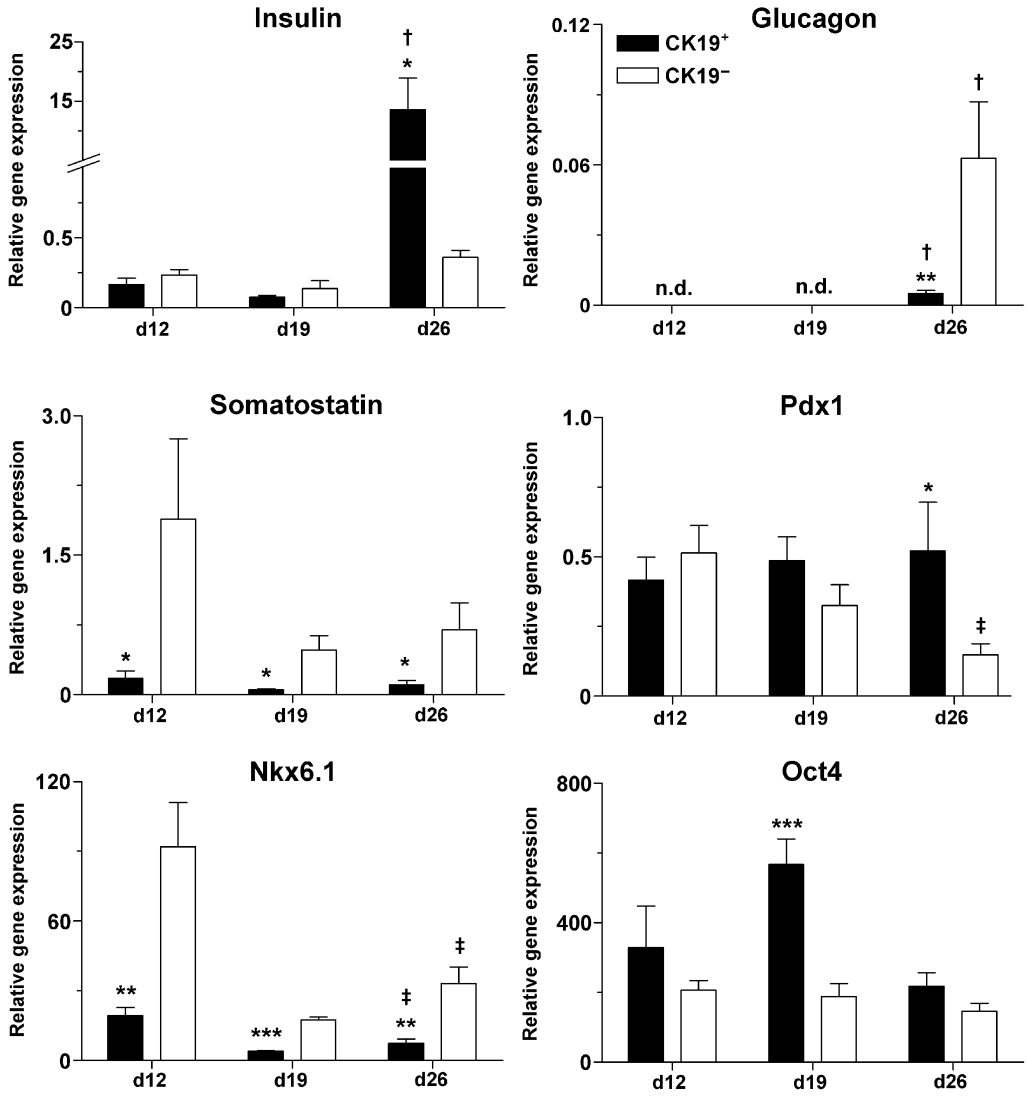

Figure 3. Comparison of the gene expression profile of pancreatic hormones insulin, glucagon and somatostatin, the transcription factors Pdx1 and Nkx6.1 and embryonic marker Oct4, in CK19$^+$ and CK19$^-$ cells, during differentiation of mouse embryonic stem cells at days 12, 19 and 26 of the optimized four-stage differentiation protocol. Values shown are means ± SEM of relative gene expression of 5–14 experiments. n.d., not detectable. *$P < 0.05$, **$P < 0.01$, ***$P < 0.001$, CK19$^+$ compared to CK19$^-$ cells. †$P < 0.05$, ‡$P < 0.01$, compared to cells on day 12.

cells can be classified as a population of monohormonal insulin-positive cells, while CK19$^-$ cells are polyhormonal cells with similar levels of glucagon and somatostatin and low insulin gene expression.

The transcription factor Pdx1, a transactivator of the insulin gene, was expressed throughout the differentiation from days 12–26 in CK19$^+$ cells, whereas its expression in CK19$^-$ cells decreased significantly from day 12–26 (Fig. 3). On day 26, Pdx1 expression in CK19$^+$ cells was 3.5 times higher than in CK19$^-$ cells. Nkx6.1, a transcription factor found in adult β-cells and during vertebrate central nervous system development, was predominantly expressed in CK19$^-$ cells,

in particular at day 12, while Nkx6.1 expression in $CK19^+$ cells was significantly lower at each time point, between four and five times, as compared to $CK19^-$ cells (Fig. 3). Oct4 was expressed in $CK19^+$ cells and $CK19^-$ cells throughout the differentiation protocol, but it decreased towards the end of the differentiation protocol at day 26 (Fig. 3).

Gene expression profile of β-cell-specific structural markers in $CK19^+$ and $CK19^-$ cells during differentiation of mouse ESCs

A significant increase in Glut2 glucose transporter and *glucokinase* gene expression was observed in $CK19^+$ and $CK19^-$ cells on day 26 as compared to day 12 and day 19 (Fig. 4). The level of *Glut2* expression was significantly higher in $CK19^+$ than in $CK19^-$ cells at day 26 (Fig. 4). Both the *Kir6.2* and *Sur1* genes, which code for ATP-sensitive potassium channel protein and the associated sulphonylurea receptor protein, were expressed throughout the whole differentiation protocol at days 12, 19 and 26 in $CK19^+$ and $CK19^-$ cells (Fig. 4).

Nestin and *NCAM* genes, which code for neuronal marker proteins, were also transcribed throughout the whole differentiation protocol at days 12, 19 and 26 in $CK19^+$ and $CK19^-$ cells (Fig. 4). Both genes were preferentially expressed in $CK19^-$ cells (Fig. 4).

Thus, β-cell-specific expression of genes for glucose-sensing proteins as well as for proteins making the β-cell depolarizing, predominated in $CK19^+$ cells, while neuron-specific gene expression prevailed in $CK19^-$ cells.

Immunocytochemical staining for C-peptide, of differentiated mouse ESCs

$CK19^+$ cells had positive staining for C-peptide and insulin in the cytoplasm with a dot-like appearance, providing evidence for ongoing active preproinsulin biosynthesis and for insulin processing, while $CK19^-$ cells were negative for C-peptide. Nonetheless, staining for insulin revealed that single $CK19^-$ cells exhibited a little immunoreactivity for insulin, albeit at very low levels, which, however, did not co-stain with C-peptide (Fig. 5a). The MIN6 insulin-producing β-cell line was used as positive control and showed distinct co-localization of C-peptide and insulin in a manner similar to $CK19^+$ cells (Fig. 6a).

Ultrastructure of differentiated mouse ESCs

$CK19^+$ cells, in contrast to undifferentiated $CK19^-$ cells, exhibited clear signs of differentiation with respect to subcellular organelles for synthesis, processing, storage and release of insulin. $CK19^-$ cells possessed fewer mitochondria and few dilated cisternae of the endoplasmatic reticulum with a minor number of ribosomes (Fig. 5b). The $CK19^+$ cells showed both well-developed rough endoplasmic reticulum and Golgi apparatus, well suited for insulin synthesis, and insulin-secretory granules, together with a high number of mitochondria providing the basis for sufficient energy supply for the cells' protein synthesis. A distinct proportion of the secretory granules were located in the vicinity of the plasma membrane with some single granules undergoing exocytosis (Fig. 5b). This was comparable to the situation that can be observed in MIN6 insulin-producing β-cells although the number of secretory granules in $CK19^+$ cells was lower than in MIN6 cells.

Insulin content in differentiated mouse ESCs

Embryonic stem cells differentiated according to the four-stage protocol contained detectable amounts of insulin (0.37 ± 0.09 ng insulin/10^6 cells, $n = 6$) in the same range as found in cells grown with the reference protocol (0.25 ± 0.07 ng insulin/10^6 cells, $n = 3$) (Fig. 7a). Analysis of the $CK19^+$ and $CK19^-$ cells revealed increased insulin content in $CK19^+$ cells. Insulin content was 50 times higher in $CK19^+$ cells (113.3 ± 37.7 ng insulin/10^6 cells, $n = 5$) compared to

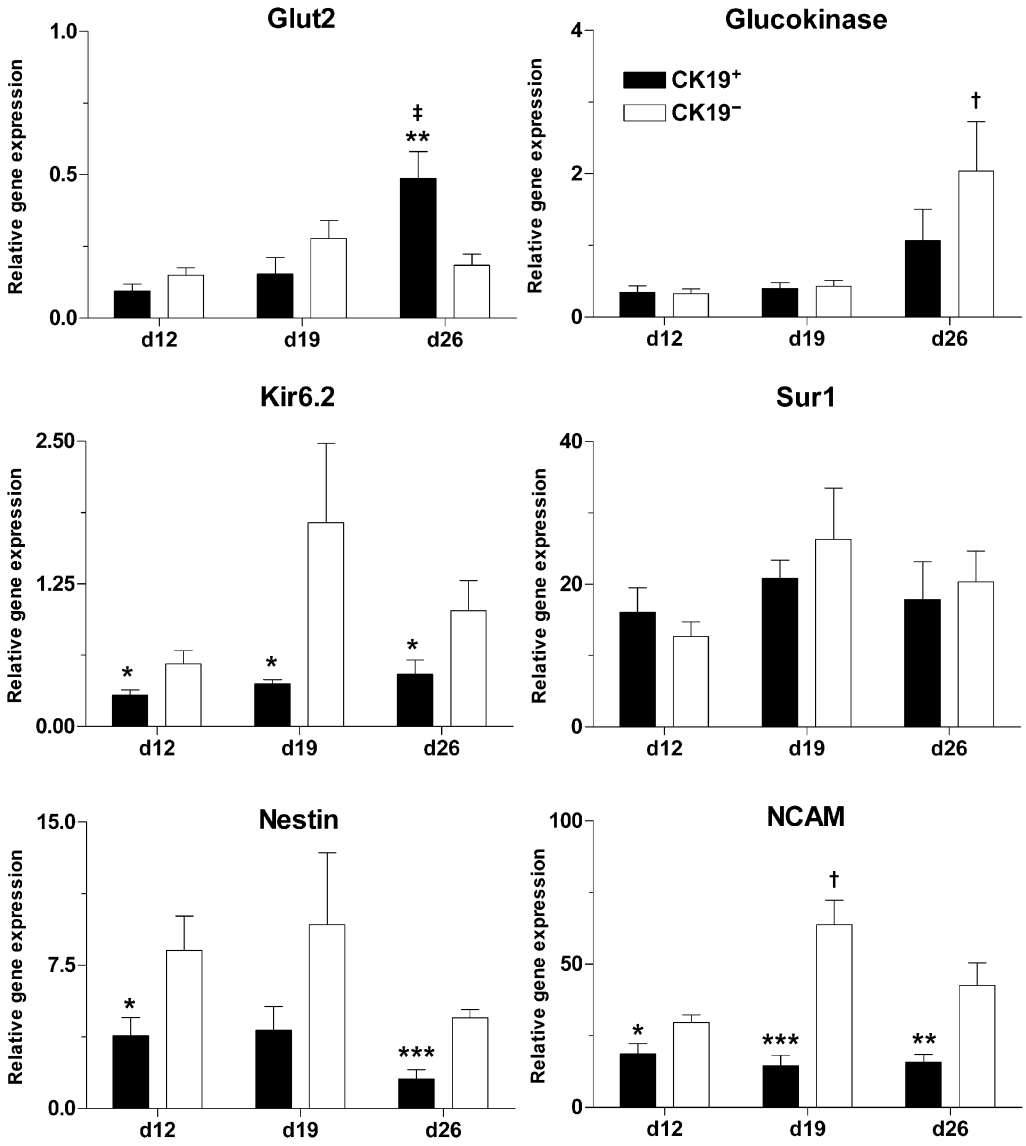

Figure 4. Comparison of gene expression profile of the structural markers Glut2 glucose transporter, glucokinase, Kir6.2, Sur1, nestin and NCAM in CK19$^+$ and CK19$^-$ cells during differentiation of mouse embryonic stem cells at days 12, 19 and 26 of the optimized four-stage differentiation protocol. Values shown are means ± SEM of the relative gene expression of five to eight experiments. *$P < 0.05$, **$P < 0.01$, ***$P < 0.001$, CK19$^+$ compared to CK19$^-$ cells. †$P < 0.05$, ‡$P < 0.01$, compared to cells on day 12. NCAM, neural cell adhesion molecule.

CK19$^-$ cells (2.1 ± 0.5 ng insulin/10^6 cells, $n = 5$) (Fig. 7a). The removal of damaged and dead cells through FACS-sorting also contributed to increased levels of insulin content in the sorted cells.

Insulin secretion in differentiated CK19$^+$ and CK19$^-$ mouse ESCs

To evaluate whether CK19$^+$ and CK19$^-$ cells release insulin in a glucose-dependent manner, insulin secretion was determined. Both groups showed the same basal insulin release at 0 mM

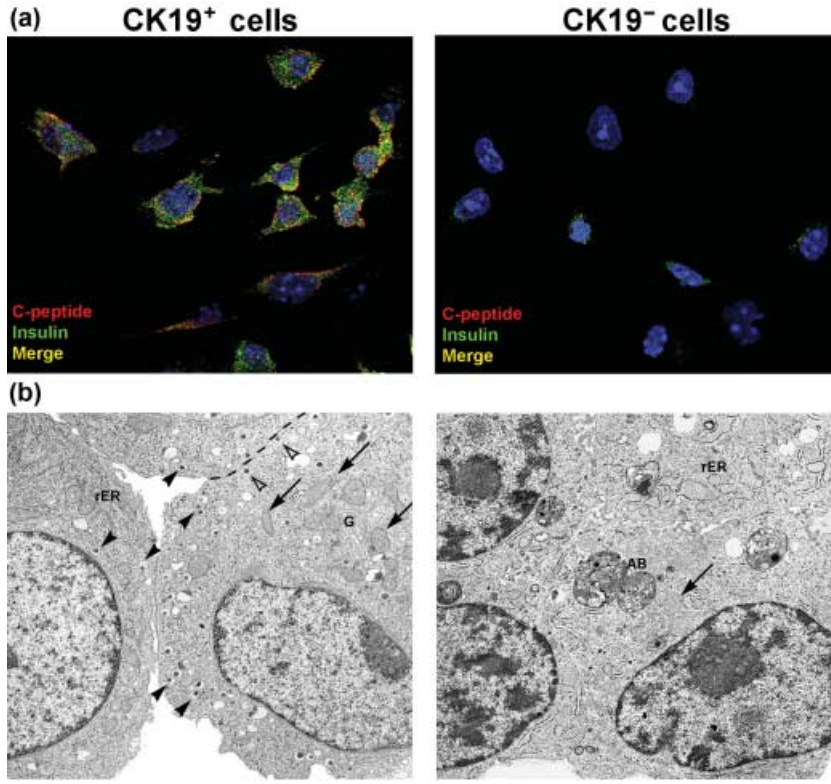

Figure 5. Comparison of C-peptide and insulin staining of CK19$^+$ and CK19$^-$ cells after differentiation of mouse embryonic stem cells (ESCs) at day 26 of the optimized four-stage differentiation protocol. Ultrastructure of CK 19$^+$ and CK19$^-$ ESCs at day 26 of the optimized four-stage differentiation protocol. (a) After FACS sorting CK19$^+$ and CK19$^-$ cells were seeded on glass slides and were stained for C-peptide (red) and insulin (green). Nuclei were counter-stained with DAPI (blue). The merge is shown in yellow. Original magnification ×600. (b) Shown on the left side is an electron micrograph of typical well-differentiated CK19$^+$ cells with characteristics of endocrine insulin-producing cells with well-developed rough endoplasmic reticulum (rER), Golgi apparatus (G) and secretory granules (*arrowheads*) and a high number of mitochondria (*arrows*). Some of the secretory granules are situated near to the plasma membrane (*dashed line*) ready for exocytosis (*open arrowheads*). On the right, shown for comparison, is an electron micrograph of CK19$^-$ cells with a small number of mitochondria (*arrows*), dilated endoplasmic reticulum and a high number of autophagic bodies (AB). Original magnification ×8000.

glucose. Incubation of CK19$^+$ cells with 30 mM glucose resulted in release of 5.0 ± 1.8 ng insulin/10^6 cells (n = 4) in 2 h, whereas CK19$^-$ cells showed no such increase (0.35 ± 0.09 ng insulin/10^6 cells, n = 5) on stimulation, when compared to basal insulin release rate (0.5 ± 0.17 ng insulin/10^6 cells, n = 5) (Fig. 7b).

DISCUSSION

Quantitative analysis of gene expression in mouse ESCs, which were differentiated according to the reference protocol by Lumelsky *et al*. (2001), showed that all three major endocrine

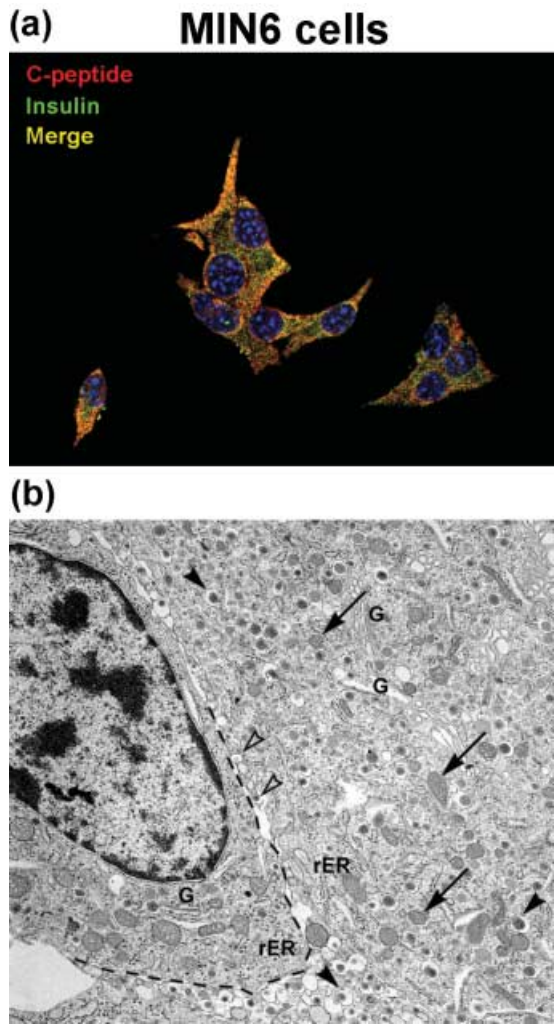

Figure 6. C-peptide and insulin staining and ultrastructure of MIN6 insulin-producing cells. (a) MIN6 cells were seeded on glass slides and were stained for C-peptide (red) and insulin (green); nuclei were counterstained with DAPI (blue). The merge is shown in yellow. Original magnification ×600. (b) The electron micrograph of MIN6 insulin-producing cells shows the typical endocrine morphology with high numbers of mitochondria (arrows), well developed rough endoplasmic reticulum (rER), Golgi apparatus (G) and secretory granules (*arrowheads*) some of them ready for exocytosis (open arrowheads). Original magnification ×8000.

hormones, insulin, glucagon and somatostatin, were readily expressed. Differentiation of ESCs according to the newly developed optimized four-stage differentiation protocol, in contrast to other published differentiation protocols (Lumelsky *et al*. 2001; Blyszczuk *et al*. 2003; Bai *et al*. 2005), yielded monohormonal insulin-producing cells, which virtually exclusively expressed insulin, with no glucagon expression and minor somatostatin expression.

Through removal of nestin selection, we produced cells with a significantly reduced neuronal character, as documented by reduction of expression levels of the neuronal markers nestin and NCAM. At the same time, β-cell-like characteristics of these insulin-producing cells were reinforced

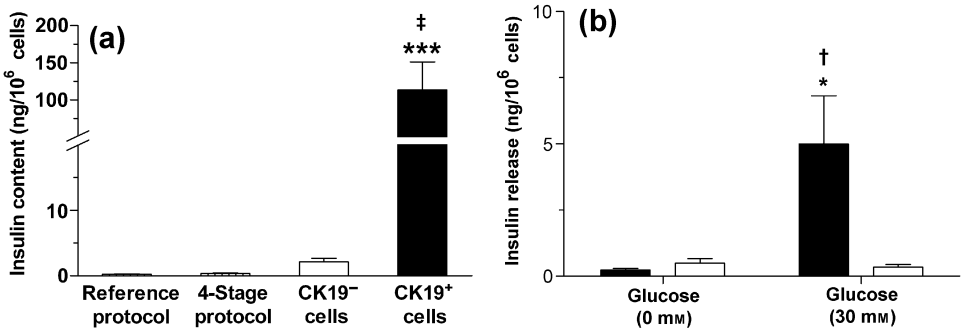

Figure 7. Comparison of insulin content of mouse embryonic stem cells after differentiation into insulin-producing cells, according to the reference differentiation protocol by Lumelsky *et al.* (2001) to the optimized four-stage differentiation protocol, as well as of the latter cells after separation into CK19$^+$ and CK19$^-$ cells. Comparison of insulin release in CK19$^+$ and CK19$^-$ cells after 2 h static incubation with 0 mM and 30 mM glucose. (a) Values shown are means ± SEM of the insulin content (ng/10^6 cells) of three to six experiments. ***$P < 0.001$, CK19$^+$ compared to CK19$^-$ cells. ‡$P < 0.01$, CK19$^+$ compared to cells from the reference protocol. (b) Values shown are means ± SEM of the insulin released (ng/10^6 cells) in 2 h of three to five experiments. *$P < 0.05$, CK19$^+$ compared to CK19$^-$ cells. †$P < 0.05$, compared to CK19$^+$ cells treated with 0 mM glucose. For comparison, insulin content of the MIN6 insulin-producing cells was 817.6 ± 123.5 ng insulin/10^6 cells, $n = 64$.

by high the gene expression level of the Glut2 glucose transporter and the transcription factor Pdx1. High levels of expression were also present for other β-cell characteristic genes, namely of the glucose sensor enzyme glucokinase as well as the potassium channel *Kir6.2* and the sulphonylurea receptor *Sur1*. In parallel, markers for differentiation towards ductal cells, namely CK19 and CA2, were significantly increased. On the other hand, lack of expression of amylase and albumin excluded significant differentiation towards exocrine pancreas and hepatic progeny.

These results support the contention that the removal of the nestin selection step from the differentiation protocol drives ESCs to the direction of insulin-producing cells and reduces neuronal characteristics of the differentiated cells. Thus, selection strategies focused on nestin expression (Lumelsky *et al*. 2001; Hori *et al*. 2002; Blyszczuk *et al*. 2003; Moritoh *et al*. 2003; Miyazaki *et al*. 2004; Bai *et al*. 2005) are not particularly suited to differentiation of ESCs into insulin-producing cells (Rajagopal *et al*. 2003; Hansson *et al*. 2004; Sipione *et al*. 2004). Not surprisingly, therefore, differentiation protocols that yielded cells with increased nestin positivity (Blyszczuk *et al*. 2003) were not significantly superior to the protocol devised by Lumelsky *et al*. (2001).

Therefore, rather than on nestin-positive cells, we focused our attention on CK19$^+$ as a selection marker for insulin-producing cells. CK19$^+$ ductal cells are generally considered to be progenitors for endocrine cells during pancreatic organogenesis (Rutter 1980; Slack 1995; Bouwens & De Blay 1996; Bouwens *et al*. 1997, 1998). *In vitro* analysis of purified CK19$^+$ cells demonstrated the capacity to proliferate and differentiate into islet cells (Bouwens *et al*. 1997, 1998, 2005; Bonner-Weir *et al*. 2000; Gao *et al*. 2003, 2005). In addition, recent work has shown that human embryonic stem cells follow, during their differentiation towards endocrine cells, the same developmental pathway known from *in vivo* development of the pancreas (D'Amour *et al*. 2005, 2006). Thus, it is clear that during *in vitro* differentiation of stem cells the last differentiation step towards β-cell type must occur *via* a CK19$^+$ cell population that expresses insulin. Moreover, the expression of CK19 as a marker of pancreatic ducts is in line with endodermal origin, and

clearly distinguishes such cells from cells of neuroectodermal progeny (Bouwens 2004; Hisatomi *et al*. 2004; Bouwens *et al*. 2005).

Following this assumption, we have on the basis of the new optimized differentiation protocol, set up a separation strategy using FACS sorting of fluorescent $CK19^+$ and non-fluorescent $CK19^-$ cells. We have used the CK19 promoter to control expression of eYFP in mouse ESCs during their differentiation towards insulin-producing cells. Previous studies have shown that the CK19 promoter is particularly potent to target duct cells (Brembeck *et al*. 2001). Two distinct cell populations, $CK19^+$ and $CK19^-$ cells, could be successfully separated and analysed using this FACS sorting procedure. Gene expression analysis of endogenous CK19 revealed that this gene is predominantly expressed in the FACS-sorted $CK19^+$ population. Thus, our selection procedure purifies ductal progenitor cells and separates them successfully from the $CK19^-$, non-ductal cell population. A detailed molecular, biochemical and morphological analysis revealed that $CK19^+$ cells represent a population of differentiated ESCs, which express the insulin prohormone gene, and process, store and release insulin.

We obtained 1.6% $CK19^+$ cells, which, in comparison with the $CK19^-$ cell fraction, had a nearly 40-fold higher level of insulin gene expression and a 50-fold higher content of insulin. This insulin content is around 450 times higher than that obtained using the reference protocol of Lumelsky *et al*. (2001) and still around 300 times higher than the optimized four-stage differentiation protocol, from which we started the CK19 separation procedure. Thus, this separation strategy of FACS sorting is far more efficient then previously published differentiation protocols (Lumelsky *et al*. 2001; Hori *et al*. 2002; Blyszczuk *et al*. 2003, 2004; Miyazaki *et al*. 2004; Bai *et al*. 2005; Shiroi *et al*. 2005).

When compared to the clonal insulin-producing cell lines RINm5F and MIN6, which like differentiated embryonic stem cells also reside in a tissue culture milieu, the level of insulin content in MIN6 insulin-producing cells is about seven times higher, and in RINm5F cells it is about 13 times lower than found in $CK19^+$ cells. Isolated islets of Langerhans, containing β-cells and other endocrine and non-endocrine cells types, lose insulin content and expression within less than 1–2 weeks (Weinberg *et al*. 2007). Thus, it is not surprising that embryonic stem cells differentiated *in vitro* towards insulin-producing cells do not reach insulin content and expression levels comparable to those of mature freshly isolated β-cells.

The $CK19^+$ cells expressed nearly 40 times more insulin but 12 times less glucagon and 7 times less somatostatin than $CK19^-$ cells. Thus, $CK19^+$ cells can be classified as monohormonal insulin-positive cells, while $CK19^-$ cells are polyhormonal cells with similar levels of glucagon and somatostatin but low insulin gene expression. In contrast to the $CK19^-$ ones, $CK19^+$ cells also exhibited a glucose-responsive insulin secretion.

Gene expression of Glut2 glucose transporter and transcription factor Pdx1 were also higher in $CK19^+$ cells. Expression levels of genes, which are known to be present both in β-cells and neuronal cells, namely of the potassium channel Kir6.2 and of the sulphonylurea receptor Sur1, were similar in both fractions, while gene expression levels of the typical neuronal markers such as nestin and NCAM were higher in $CK19^-$ cells. This is in accordance with the observation that NCAM is significantly expressed only in pancreatic α-cells while it is low in β-cells and absent in acinar and duct cells (Cirulli *et al*. 1994). The significantly higher expression of the transcription factor Nkx6.1 in $CK19^-$ cells supports the contention that this is also a gene with primary importance for neuronal development (Liu *et al*. 2003; Przyborski *et al*. 2003). This provides further support for the hypothesis that differentiation *via* neuronal precursors does not generate insulin-producing cells. $CK19^+$ cells exhibit the typical characteristics of pancreatic β-cells. In contrast to the $CK19^-$ cell population, $CK19^+$ cells are also C-peptide and insulin-positive and show, on ultrastructural analysis, typical characteristics of insulin-secretory cells, namely well-developed rough

endoplasmic reticulum, Golgi apparatus and secretory granules. Thus, the small proportion of C-peptide-positive cells that have been reported after ESCs had passed through differentiation protocols towards insulin-producing cells (Blyszczuk *et al*. 2004; Paek *et al*. 2005) can be considered to be the source of the C-peptide-positive cells with typical ultrastructural characteristics of secretory cells, which we have found in the present study in the fraction of the $CK19^+$ cells.

During the course of differentiation from ESCs towards insulin-producing cells, a fraction of the cells undergoes cell death through apoptosis. Thus, at the end of the differentiation procedure, the cell population contains a proportion of dead cells (Rajagopal *et al*. 2003; Hansson *et al*. 2004; Sipione *et al*. 2004; Duval *et al*. 2006). These apoptotic cells are particularly prone to uptake of insulin from the extracellular space (Rajagopal *et al*. 2003). This can lead to overestimation of the efficiency of a differentiation protocol (Hansson *et al*. 2004). However, because differentiation culture media require insulin supplementation for proper proliferation of the cells, it is necessary to separate the dead cells from the total cell population. Therefore, this separation-out of dead cells is part of our FACS sorting procedure (Fig. 2). Thus, the obtained populations of $CK19^+$ and $CK19^-$ cells were not contaminated with apoptotic cells, excluding an overestimation of cellular insulin content due to uptake from the differentiation medium.

In conclusion, our results show that this combined procedure is suitable for obtaining C-peptide-positive, glucose-responsive insulin-secreting $CK19^+$ cells. That the population of insulin-positive cells are, in addition, positive for CK19, provides strong support for the concept of ductal origin of insulin-producing cells (Bonner-Weir *et al*. 2000, 2004; Gao *et al*. 2003, 2005; Bouwens *et al*. 2005). Thus, these cells represent an endocrine precursor cell type with typical ultrastructural characteristics of insulin-secretory cells, potentially suitable for insulin replacement therapy in diabetes.

ACKNOWLEDGEMENTS

This work was supported by the European Union (project QLK3-CT-2002-01777) in the Framework Programme 5 and the Excellence Cluster REBIRTH (Deutsche Forschungsgemeinschaft).

REFERENCES

Bai L, Meredith G, Tuch BE (2005) Glucagon-like peptide-1 enhances production of insulin in insulin-producing cells derived from mouse embryonic stem cells. *J. Endocrinol*. **186**, 343–352.

Blyszczuk P, Asbrand C, Rozzo A, Kania G, St-Onge L, Rupnik M, Wobus AM (2004) Embryonic stem cells differentiate into insulin-producing cells without selection of nestin-expressing cells. *Int. J. Dev. Biol*. **48**, 1095–1104.

Blyszczuk P, Czyz J, Kania G, Wagner M, Roll U, St-Onge L, Wobus AM (2003) Expression of Pax4 in embryonic stem cells promotes differentiation of nestin-positive progenitor and insulin-producing cells. *Proc. Natl. Acad. Sci. USA* **100**, 998–1003.

Bonner-Weir S, Taneja M, Weir GC, Tatarkiewicz K, Song KH, Sharma A, O'Neil JJ (2000) *In vitro* cultivation of human islets from expanded ductal tissue. *Proc. Natl. Acad. Sci. USA* **97**, 7999–8004.

Bonner-Weir S, Toschi E, Inada A, Reitz P, Fonseca SY, Aye T, Sharma A (2004) The pancreatic ductal epithelium serves as a potential pool of progenitor cells. *Pediatr. Diabetes* **5** (Suppl. 2), 16–22.

Bouwens L (2004) Islet morphogenesis and stem cell markers. *Cell Biochem. Biophys*. **40**, 81–88.

Bouwens L, De Blay E (1996) Islet morphogenesis and stem cell markers in rat pancreas. *J. Histochem. Cytochem*. **44**, 947–951.

Bouwens L, Lu WG, De Krijger R (1997) Proliferation and differentiation in the human fetal endocrine pancreas. *Diabetologia* **40**, 398–404.

Bouwens L, Pipeleers DG (1998) Extra-insular beta cells associated with ductules are frequent in adult human pancreas. *Diabetologia* **41**, 629–633.

Bouwens L, Rooman I (2005) Regulation of pancreatic β-cell mass. *Physiol. Rev*. **85**, 1255–1270.

Brembeck FH, Moffett J, Wang TC, Rustgi AK (2001) The keratin 19 promoter is potent for cell-specific targeting of genes in transgenic mice. *Gastroenterology* **120**, 1720–1728.

Chomczynski P, Sacchi N (1987) Single-step method of RNA isolation by acid guanidinium thiocyanate-phenol-chloroform extraction. *Anal. Biochem*. **162**, 156–159.

Cirulli V, Baetens D, Rutishauser U, Halban PA, Orci L, Rouiller DG (1994) Expression of neural cell adhesion molecule (NCAM) in rat islets and its role in islet cell type segregation. *J. Cell. Sci*. **107**, 1429–1436.

D'Amour KA, Agulnick AD, Eliazer S, Kelly OG, Kroon E, Baetge EE (2005) Efficient differentiation of human embryonic stem cells to definitive endoderm. *Nat. Biotechnol*. **23**, 1534–1541.

D'Amour KA, Bang AG, Eliazer S, Kelly OG, Agulnick AD, Smart NG, Moorman MA, Kroon E, Carpenter MK, Baetge EE (2006) Production of pancreatic hormone-expressing endocrine cells from human embryonic stem cells. *Nat. Biotechnol*. **24**, 1392–1401.

Doetschman TC, Eistetter H, Katz M, Schmidt W, Kemler R (1985) The *in vitro* development of blastocyst-derived embryonic stem cell lines: formation of visceral yolk sac, blood islands and myocardium. *J. Embryol. Exp. Morph*. **87**, 27–45.

Duval D, Trouillas M, Thibault C, Dembele D, Diemunsch F, Reinhardt B, Mertz AL, Dierich A, Boeuf H (2006) Apoptosis and differentiation commitment: novel insights revealed by gene profiling studies in mouse embryonic stem cells. *Cell Death Differ*. **13**, 564–575.

Edlund H (2002) Pancreatic organogenesis-developmental mechanisms and implications for therapy. *Nat. Rev. Genet*. **3**, 524–532.

Gao R, Ustinov J, Korsgren O, Otonkoski T (2005) *In vitro* neogenesis of human islets reflects the plasticity of differentiated human pancreatic cells. *Diabetologia* **48**, 2296–2304.

Gao R, Ustinov J, Pulkkinen MA, Lundin K, Korsgren O, Otonkoski T (2003) Characterization of endocrine progenitor cells and critical factors for their differentiation in human adult pancreatic cell culture. *Diabetes* **52**, 2007–2015.

Gmyr V, Kerr-Conte J, Belaich S, Vandewalle B, Leteurtre E, Vantyghem MC, Lecomte-Houcke M, Proye C, Lefebvre J, Pattou F (2000) Adult human cytokeratin 19-positive cells reexpress insulin promoter factor 1 *in vitro*: further evidence for pluripotent pancreatic stem cells in humans. *Diabetes* **49**, 1671–1680.

Gurgul E, Lortz S, Tiedge M, Jorns A, Lenzen S (2004) Mitochondrial catalase overexpression protects insulin-producing cells against toxicity of reactive oxygen species and proinflammatory cytokines. *Diabetes* **53**, 2271–2280.

Hansson M, Tonning A, Frandsen U, Petri A, Rajagopal J, Englund MC, Heller RS, Hakansson J, Fleckner J, Skold HN, Melton D, Semb H, Serup P (2004) Artifactual insulin release from differentiated embryonic stem cells. *Diabetes* **53**, 2603–2609.

Hisatomi Y, Okumura K, Nakamura K, Matsumoto S, Satoh A, Nagano K, Yamamoto T, Endo F (2004) Flow cytometric isolation of endodermal progenitors from mouse salivary gland differentiate into hepatic and pancreatic lineages. *Hepatology* **39**, 667–675.

Hori Y, Rulifson IC, Tsai BC, Heit JJ, Cahoy JD, Kim SK (2002) Growth inhibitors promote differentiation of insulin-producing tissue from embryonic stem cells. *Proc. Natl. Acad. Sci. USA* **99**, 16105–16110.

Hunziker E, Stein M (2000) Nestin-expressing cells in the pancreatic islets of Langerhans. *Biochem. Biophys. Res. Commun*. **271**, 116–119.

Jiang J, Au M, Lu K, Eshpeter A, Korbutt G, Fisk G, Majumdar AS (2007) Generation of insulin-producing islet-like clusters from human embryonic stem cells. *Stem Cells* **25**, 1940–1953.

Lee SH, Lumelsky N, Studer L, Auerbach JM, McKay RD (2000) Efficient generation of midbrain and hindbrain neurons from mouse embryonic stem cells. *Nat. Biotechnol*. **18**, 675–679.

Leon-Quinto T, Jones J, Skoudy A, Burcin M, Soria B (2004) *In vitro* directed differentiation of mouse embryonic stem cells into insulin-producing cells. *Diabetologia* **47**, 1442–1451.

Liu R, Cai J, Hu X, Tan M, Qi Y, German M, Rubenstein J, Sander M, Qiu M (2003) Region-specific and stage-dependent regulation of Olig gene expression and oligodendrogenesis by Nkx6.1 homeodomain transcription factor. *Development* **130**, 6221–6231.

Lumelsky N, Blondel O, Laeng P, Velasco I, Ravin R, McKay R (2001) Differentiation of embryonic stem cells to insulin-secreting structures similar to pancreatic islets. *Science* **292**, 1389–1394.

Miyazaki J, Araki K, Yamato E, Ikegami H, Asano T, Shibasaki Y, Oka Y, Yamamura K (1990) Establishment of a pancreatic β-cell line that retains glucose-inducible insulin secretion: special reference to expression of glucose transporter isoforms. *Endocrinology* **127**, 126–132.

Miyazaki S, Yamato E, Miyazaki J (2004) Regulated expression of Pdx-1 promotes *in vitro* differentiation of insulin-producing cells from embryonic stem cells. *Diabetes* **53**, 1030–1037.

Moritoh Y, Yamato E, Yasui Y, Miyazaki S, Miyazaki J (2003) Analysis of insulin-producing cells during *in vitro* differentiation from feeder-free embryonic stem cells. *Diabetes* **52**, 1163–1168.

Muller PY, Janovjak H, Miserez AR, Dobbie Z (2002) Processing of gene expression data generated by quantitative real-time RT-PCR. *Biotechniques* **32**, 1372–1374, 1376, 1378–1379.

Noguchi H, Kaneto H, Weir GC, Bonner-Weir S (2003) PDX-1 protein containing its own antennapedia-like protein transduction domain can transduce pancreatic duct and islet cells. *Diabetes* **52**, 1732–1737.

Paek HJ, Morgan JR, Lysaght MJ (2005) Sequestration and synthesis: the source of insulin in cell clusters differentiated from murine embryonic stem cells. *Stem Cells* **23**, 862–867.

Przyborski SA, Smith S, Wood A (2003) Transcriptional profiling of neuronal differentiation by human embryonal carcinoma stem cells *in vitro*. *Stem Cells* **21**, 459–471.

Rajagopal J, Anderson WJ, Kume S, Martinez OI, Melton DA (2003) Insulin staining of ES cell progeny from insulin uptake. *Science* **299**, 363.

Ramakers C, Ruijter JM, Deprez RH, Moorman AF (2003) Assumption-free analysis of quantitative real-time polymerase chain reaction (PCR) data. *Neurosci. Lett*. **339**, 62–66.

Roche E, Sepulcre P, Reig JA, Santana A, Soria B (2005) Ectodermal commitment of insulin-producing cells derived from mouse embryonic stem cells. *FASEB J*. **19**, 1341–1343.

Rutter WJ (1980) The development of the endocrine and exocrine pancreas. *Monogr. Pathol*. **21**, 30–38.

Selander L, Edlund H (2002) Nestin is expressed in mesenchymal and not epithelial cells of the developing mouse pancreas. *Mech. Dev*. **113**, 189–192.

Shi Y, Hou L, Tang F, Jiang W, Wang P, Ding M, Deng H (2005) Inducing embryonic stem cells to differentiate into pancreatic beta cells by a novel three-step approach with activin A and all-trans retinoic acid. *Stem Cells* **23**, 656–662.

Shiroi A, Ueda S, Ouji Y, Saito K, Moriya K, Sugie Y, Fukui H, Ishizaka S, Yoshikawa M (2005) Differentiation of embryonic stem cells into insulin-producing cells promoted by Nkx2.2 gene transfer. *World J. Gastroenterol*. **11**, 4161–4166.

Sipione S, Eshpeter A, Lyon JG, Korbutt GS, Bleackley RC (2004) Insulin expressing cells from differentiated embryonic stem cells are not β-cells. *Diabetologia* **47**, 499–508.

Slack JM (1995) Developmental biology of the pancreas. *Development* **121**, 1569–1580.

Soria B, Roche E, Berna G, Leon-Quinto T, Reig JA, Martin F (2000) Insulin-secreting cells derived from embryonic stem cells normalize glycemia in streptozotocin-induced diabetic mice. *Diabetes* **49**, 157–162.

Treutelaar MK, Skidmore JM, Dias-Leme CL, Hara M, Zhang L, Simeone D, Martin DM, Burant CF (2003) Nestin-lineage cells contribute to the microvasculature but not endocrine cells of the islet. *Diabetes* **52**, 2503–2512.

Vaca P, Martin F, Vegara-Meseguer JM, Rovira JM, Berna G, Soria B (2006) Induction of differentiation of embryonic stem cells into insulin-secreting cells by fetal soluble factors. *Stem Cells* **24**, 258–265.

Weinberg N, Ouziel-Yahalom L, Knoller S, Efrat S, Dor Y (2007) Lineage tracing evidence for *in vitro* dedifferentiation but rare proliferation of mouse pancreatic β-cells. *Diabetes* **56**, 1299–1304.

Zulewski H, Abraham EJ, Gerlach MJ, Daniel PB, Moritz W, Muller B, Vallejo M, Thomas MK, Habener JF (2001) Multipotential nestin-positive stem cells isolated from adult pancreatic islets differentiate *ex vivo* into pancreatic endocrine, exocrine, and hepatic phenotypes. *Diabetes* **50**, 521–533.

